



1           **Estimating Surface Carbon Fluxes Based on a Local Ensemble**  
2           **Transform Kalman Filter with a Short Assimilation Window and a**  
3                           **Long Observation Window**

4  
5     <sup>1</sup>Yun Liu, <sup>1</sup>Eugenia Kalnay\*, <sup>1</sup>Ning Zeng, <sup>2</sup>Ghassem Asrar, <sup>3</sup>Zhaohui Chen, <sup>4</sup>Binghao Jia

6  
7           1 Dept. of Atmospheric and Oceanic Science, University of Maryland – College Park

8                     2 Joint Global Change Research Institute/PNNL, College Park, MD

9                     3 School of Environmental Science, University of East Anglia, Norwich, UK

10                    4 State Key Laboratory of Numerical Modeling for Atmospheric Sciences and  
11                    Geophysical Fluid Dynamics (LASG), Institute of Atmospheric Physics, Chinese  
12                    Academy of Sciences, Beijing, China

13  
14     \*Corresponding author

15  
16  
17  
18  
19  
20  
21  
22  
23  
24  
25  
26  
27  
28  
29  
30  
31  
32  
33  
34  
35  
36  
37  
38  
39  
40  
41  
42  
43  
44



1 **Abstract**

2 We developed a Carbon data assimilation system to estimate the surface carbon  
3 fluxes using the Local Ensemble Transform Kalman Filter and atmospheric transfer  
4 model of GEOS-Chem driven by the MERRA-1 reanalysis of the meteorological fields  
5 based on the Goddard Earth Observing System Model, Version 5 (GEOS-5). This  
6 assimilation system is inspired by the method of Kang et al. [2011, 2012], who estimated  
7 the surface carbon fluxes in an Observing System Simulation Experiment (OSSE) mode,  
8 as evolving parameters in the assimilation of the atmospheric CO<sub>2</sub>, using a short  
9 assimilation window of 6 hours. They included the assimilation of the standard  
10 meteorological variables, so that the ensemble provided a measure of the uncertainty in  
11 the CO<sub>2</sub> transport. After introducing new techniques such as “variable localization”, and  
12 increased observation weights near the surface, they obtained accurate carbon fluxes at  
13 grid point resolution. We developed a new version of the LETKF related to the  
14 “Running-in-Place” (RIP) method used to accelerate the spin-up of EnKF data  
15 assimilation [Kalnay and Yang, 2010; Wang et al., 2013, Yang et al., 2014]. Like RIP,  
16 the new assimilation system uses the “no-cost smoothing” algorithm for the LETKF  
17 [Kalnay et al., 2007b], which allows shifting at no cost the Kalman Filter solution  
18 forward or backward within an assimilation window. In the new scheme a long  
19 “observation window” (e.g., 7-days or longer) is used to create an LETKF ensemble at 7-  
20 days. Then, the RIP smoother is used to obtain an accurate final analysis at 1-day. This  
21 analysis has the advantage of being based on a short assimilation window, which makes it  
22 more accurate, and of having been exposed to the future 7-days observations, which  
23 accelerates the spin up. The assimilation and observation windows are then shifted  
24 forward by one day, and the process is repeated. This reduces significantly the analysis  
25 error, suggesting that this method could be used in other data assimilation problems. The  
26 newly developed assimilation method can be used with other Earth system models,  
27 especially for greater use of observations in conjunction with models.

28

29

30 Key words: Carbon Data Assimilation, Surface Carbon Flux, LETKF

31



1

2

3

4

## 1. Introduction

5           The exchange of carbon among atmosphere, land and oceans contributes to  
6 changes in the Earth's climate, and is also sensitive to climate conditions. The CO<sub>2</sub>  
7 concentration in the atmosphere is affected by both the natural variability of the Earth's  
8 planetary system, and anthropogenic emissions. The terrestrial and oceanic ecosystems  
9 absorb more than one-half of the atmospheric anthropogenic CO<sub>2</sub> emission [Le Quéré *et*  
10 *al.*, 2016]. It is thus essential to quantify the dynamics of earth surface carbon fluxes  
11 (SCF), and the variations of carbon sources and sinks.

12           A common approach for estimating SCF from atmospheric CO<sub>2</sub> measurements  
13 and atmospheric transport models is referred to as a “top-down” approach. The “top-  
14 down” methods estimate SCF through techniques such as Bayesian synthesis approach  
15 [Rödenbeck *et al.*, 2003; Gurney *et al.*, 2004; Enting, 2002; Bousquet *et al.*, 1999],  
16 different types of ensemble Kalman filters (EnKF) [e.g. Peters *et al.*, 2005, 2007; Feng *et*  
17 *al.*, 2009; Zupanski *et al.* 2007; Lokupitiya *et al.*, 2008], or variational data assimilation  
18 method [e.g., Baker *et al.*, 2006, 2010; Chevallier *et al.*, 2009].

19           Kang *et al.* [2011, 2012] developed a “top-down” carbon data assimilation system  
20 by coupling an atmospheric general circulation model (AGCM), including atmospheric  
21 CO<sub>2</sub> concentrations, with the Local Ensemble Transform Kalman Filter (LETKF) [Hunt  
22 *et al.*, 2007]. The meteorological variables (wind, temperature, humidity, surface  
23 pressure) and CO<sub>2</sub> concentrations were assimilated simultaneously in order to include the  
24 uncertainties of meteorological field, and their impact on the transport of atmospheric  
25 CO<sub>2</sub>. They carried out Observing System Simulation Experiments (OSSEs), and their  
26 carbon assimilation system achieved for the first time an accurate estimation of the  
27 evolving SCF at the model grid resolution, without requiring any *a priori* information.  
28 The carbon surface fluxes were obtained from the data assimilation as “unobserved  
29 evolving parameters”, by augmenting the state vector at each column with a surface  
30 carbon flux (SCF). The Local Ensemble Transform Kalman Filter (LETKF) then  
31 estimated this evolving parameter from the error covariance between the low level  
32 atmospheric CO<sub>2</sub> and the estimated SCF, and after a spin-up of about one month, the



1 LETKF accurately recovered the nature run seasonal surface carbon fluxes.

2 Kang et al., [2011, 2012] used a short 6-hour assimilation window for both  
3 atmospheric and CO<sub>2</sub> observations because atmospheric observations are usually  
4 assimilated at this frequency, and because all Ensemble Kalman Filters require short  
5 windows to ensure that the forecast perturbations growth remains linear. Such short data  
6 assimilation, required by the LETKF, also protects the system from becoming ill  
7 conditioned [Enting, 2002, Fig. 1.3], and as a result it does not require additional *a priori*  
8 information.

9 We note that the use of such short assimilation window differs very much from  
10 most other “top-down” approaches for estimating SCF that use long assimilation  
11 windows varying from a few weeks to months [e.g., Baker et al., 2006, 2010; Peters et  
12 al., 2005, 2007; Michalak, 2008; Feng et al., 2009].

13 Although the Kang et al. methodology was successful, it is computationally  
14 expensive, requiring ensemble forecasts and data assimilation not only for the carbon  
15 variables, but also for the standard atmospheric variables, in order to estimate the  
16 uncertainties of the CO<sub>2</sub> atmospheric transport process. In this study, we used an LETKF  
17 carbon cycle data assimilation system with a state-of-the-art atmospheric transport model,  
18 the GEOS-Chem [Bey et al., 2001; Nassar et al., 2013], which is driven by the MERRA-1  
19 reanalysis of the Goddard Earth Observing System Model, Version 5 (GEOS5). As a  
20 result, our system, unlike Kang et al [2011, 2012] does not include an estimation of  
21 transport uncertainties related to the meteorological field.

22 The ultimate goal of our LETKF\_C system is to estimate the grid-point SCFs,  
23 which, as in Kang et al. [2011, 2012], are treated like time-evolving parameters in the  
24 system. As mentioned before, an Ensemble Kalman Filter requires a short assimilation  
25 window in order to have the ensemble perturbations evolve linearly and remain Gaussian.  
26 On the other hand, it is well known that the training needed to estimate evolving  
27 parameters through data assimilation could be quite long, so that it benefits from having  
28 many observations. Therefore, a short assimilation window would slow down the training  
29 needed for the estimation of the SCF error covariance, and hence lengthen the spin-up  
30 time.

31 To address this problem, we developed a new version of the LETKF related to the



1 “Running-in-Place” (RIP) method used to accelerate the spin-up of EnKF data  
2 assimilation [Kalnay and Yang, 2010; Wang et al., 2013; Yang et al., 2012]. Like RIP, it  
3 uses the “no-cost smoothing” algorithm for the LETKF [Kalnay et al., 2007b] that allows  
4 shifting at a negligible cost the Kalman Filter solution forward or backward within a  
5 given assimilation window. Briefly, the new scheme works like this: a long “observation  
6 window” (e.g., 7-days, containing all the observations within 7 days) is used to create a  
7 temporary LETKF ensemble analysis at 7-days. Then the RIP smoother is used to obtain  
8 a final analysis at 1-day. This analysis has the advantage of being based on a short  
9 assimilation window, which makes it more accurate, and of having been exposed to the 7-  
10 days of observations, which accelerates the spin up time. The assimilation and  
11 observation windows are then shifted forward by one day, and the process is repeated.  
12 We have tested this new method (short assimilation, long observation window) achieving  
13 a significant reduction of analysis errors, and we believe that the method could be useful  
14 in other data assimilation problems.

15 This paper is organized as follows: Section 2 briefly describes the LETKF\_C  
16 system. Section 3 explores the effect of combing assimilation and observation windows  
17 in an OSSE framework. Section 4 presents results on the proposed methodology. A  
18 summary and discussion are presented in section 5.

19

## 20 **2. LETKF\_C data assimilation system**

21 A data assimilation system includes a forecast model, observations, and a data  
22 assimilation method that optimally combines them. In the proposed LETKF\_C data  
23 assimilation system we use the GEOS-Chem as the forecast model and LETKF as the  
24 data assimilation method. The pseudo-observations of our OSSE experiments are created  
25 at the locations of the real carbon observations retrieved from Orbiting Carbon  
26 Observatory-2 (OCO-2) satellite [Crisp et al., 2004].

27

### 28 **2.1 GEOS-Chem model and the “nature” run**

29 GEOS-Chem is a global 3-D atmospheric Chemical transport model driven by the  
30 NASA reanalysis (MERRA-1) of meteorological fields from the Goddard Earth  
31 Observing System data assimilation System Version 5, by the NASA Global Modeling



1 and Assimilation Office [Bosilovich et al., 2015]. This model has been applied  
2 worldwide to a wide range of atmospheric composition and transport studies. The  
3 GEOS-Chem model used in this study is the version v10-01 with a resolution of  $4^\circ \times 5^\circ$   
4 (latitude  $\times$  longitude), and 47 hybrid pressure-sigma vertical levels for CO<sub>2</sub> simulation  
5 [Nassar et al., 2013]. GEOS-Chem is driven by the MERRA-1 reanalysis with 72 hybrid  
6 vertical levels, extending from the surface up to 0.01 hPa. The data is provided by the  
7 GEOS-Chem support team, based at the Harvard and Dalhousie Universities with support  
8 from the NASA Earth Science Division and the Canadian National and Engineering  
9 Research Council, who re-gridded the original data of spatial resolution of  $0.25^\circ \times$   
10  $0.3125^\circ$  into the resolution of  $4^\circ \times 5^\circ$ .

11 GEOS-Chem requires the SCFs as a set of parameters at each grid point in order  
12 to simulate the CO<sub>2</sub> concentration in the atmosphere. It is not possible to observe the  
13 global SCFs directly. Therefore, the SCFs are created from a “bottom-up” approach (used  
14 as “truth” in our experiments) and used for the simulation of atmospheric CO<sub>2</sub>  
15 concentration with GEOS-Chem. The “bottom-up” SCFs used in this study include the  
16 three components shown in Equation (1): 1) terrestrial carbon fluxes ( $F_{ta}$ ); 2) air-sea  
17 carbon fluxes ( $F_{oa}$ ); 3) anthropogenic fossil fuel emissions ( $F_{fe}$ ).

$$18 \quad SCF = F_{ta} + F_{oa} + F_{fe} \quad (1)$$

19 The  $F_{ta}$  values are derived from the VEgetation Global Atmosphere Soils (VEGAS)  
20 model [Zeng et al., 2004; Zeng et al., 2005], forced by the real evolving weather, as given  
21 by the GEOS-Chem. The  $F_{oa}$  values are from Takahashi et al. [2002], a climatological  
22 seasonal cycle estimated for the 1990s, and the  $F_{fe}$  values are from Fossil Fuel Data  
23 Assimilation System (FFDAS) for the year 2012 [Asefi-Najafabady et al., 2014]. The air-  
24 sea carbon flux and  $F_{fe}$  values were scaled using the global carbon budget data of Le  
25 Quéré et al. [2015], in order to include interannual variations. A nature run for  
26 atmospheric CO<sub>2</sub> concentration simulation is driven by the SCFs in units of  $\left(\frac{kgC}{m^2yr}\right)$  based  
27 on all three datasets.

28 In OSSEs, the nature run serves as the “truth”. We assume that the true “bottom-  
29 up” carbon fluxes are not known in our data assimilation experiments, and they will be  
30 estimated using the atmospheric pseudo-observations derived from the “truth”, as  
31 described in more details below. The nature run obtained by coupling GEOS-CHEM with



1 VEGAS is fairly realistic [Liu et al., 2017], so we use it to create the pseudo OCO-2  
2 observations for the period of January 2015- March 2016.

### 3 **2.2 Pseudo-Observations**

4 The ultimate goal of this model-data assimilation system is to estimate the SCFs  
5 at every land grid point using real observations such as the conventional surface CO<sub>2</sub>  
6 measurements of GlobalViewplus (GV+) flask network provided by Cooperative Global  
7 Atmospheric Data Integration Project [2016], and the carbon observations from satellites  
8 such as the Greenhouse Gases Observing Satellite (GOSAT) [Yokota et al., 2004], and  
9 the Orbiting Carbon Observatory-2 (OCO-2) [Crisp et al., 2004]. In this study, we use  
10 the actual OCO-2 observations locations to develop the pseudo-observations for the  
11 OSSE assimilation experiments.

12 The actual OCO-2 observations cover the entire globe once every 14 days with  
13 very high spatial resolution (i.e.,  $\sim 1$  km<sup>2</sup>). The observations are the CO<sub>2</sub> column-  
14 averaged dry air mole fractions over the entire OCO-2 pixel (defined as X<sub>co2</sub>). The  
15 observation quality is greatly affected by conditions such as cloud cover, surface type and  
16 the solar zenith angle at the time of measurement. The OCO-2 retrieval algorithm uses a  
17 warning level (WL) between 0 and 19, to indicate the quality of measurements, where  
18 WL=0 means “most likely good”, and WL=19 means “least likely good” observations.  
19 The OCO-2 observations used in this study were provided by David Baker (personal  
20 communication) who averaged the original high spatial resolution observation into the  
21 coarse spatial resolution of  $\sim 1$  degree, with an average of 10-second time window, using  
22 the “good quality” observations retrieval defined by WL  $\leq 15$ . We further aggregated  
23 these observations at the nearest GEOS-Chem output time of the 0, 6, 12, 18 UTC for  
24 each model day. The actual location, time and error scales of the OCO-2 observations  
25 were then used to create the pseudo-observations. The typical one-day coverage of  
26 observation of OCO-2 is shown in Figure 1. The values of X<sub>co2</sub> in the winter are  
27 significantly larger than those in summer of the Northern hemisphere. The OCO-2  
28 observations are missing in the winter, for middle and high latitude regions (latitude  $>$   
29  $\sim 30$ ). The pseudo-observations are then created by obtaining the “true” CO<sub>2</sub> from the  
30 “nature” run using the location and time of the valid observation, and then adding random  
31 errors with due consideration to the scales of the corresponding real observations. These



1 derived pseudo-observations are more realistic than the GOSAT observations used in  
 2 Kang et al. [2012], because they are anchored to the original OCO-2 observations and to  
 3 their quality.

4

### 5 **2.3 The LETKF data assimilation system**

6 The ensemble Kalman filter (EnKF) is a powerful tool for data assimilation that  
 7 was first introduced by Evensen [1994]. The key element of this method is to derive  
 8 the forecast uncertainties from an ensemble of integrated model simulations. A  
 9 variety of ensemble Kalman filter assimilation methods have been proposed [Burgers et  
 10 al., 1998; Houtekamer and Mitchell, 1998; Anderson, 2001, 2003; Bishop et al., 2001;  
 11 Whitaker and Hamill, 2002; Tippett et al., 2003; Ott et al., 2004, Hunt et al., 2004]. The  
 12 local ensemble transform Kalman filter (LETKF) introduced by Hunt et al. [2007] is  
 13 chosen for this study.

14 The LETKF is an extension of the Local Ensemble Kalman Filter [Ott et al.,  
 15 2004] with the implementation of the ensemble transform filter [Bishop et al., 2001;  
 16 Wang and Bishop, 2003]. It is widely used for data assimilation, including several  
 17 operational centers, and was also used for carbon data assimilations by Kang et al. [2011,  
 18 2012].

19 As discussed earlier, we follow Kang et al., [2011] in estimating the SCFs as  
 20 evolving parameters, augmenting the state vector  $C$  (the prognostic variable of  
 21 atmospheric CO<sub>2</sub>) with the parameter SCF, i.e.,  $X = [C, SCF]^T$ . The analysis mean  $\bar{X}^a$   
 22 and its ensemble perturbations  $X^a$  are determined by Equations (2.1 and 2.2) at every grid  
 23 point, and the ensemble analysis is used as initial conditions for the ensemble forecast in  
 24 the next cycle.

$$25 \quad \bar{X}^a = \bar{X}^b + X^b \tilde{K} (y^o - \bar{y}^b) \quad (2.1)$$

$$26 \quad X^a = X^b [(K - 1)\tilde{P}^a]^{1/2} \quad (2.2)$$

27 Here  $\bar{X}^b$  is the ensemble mean of the forecast (background) ensemble members;  
 28  $X^b$  is a matrix whose columns are the background perturbations of  $X_k^b - \bar{X}^b$  for each  
 29 ensemble member  $X_k^b$  ( $k=1, \dots, K$ ), where  $K$  is the ensemble size);  $y^o$  is a vector of all the  
 30 observations;  $\bar{y}^b$  is the background ensemble mean in observation space ( $\bar{y}^b = H(\bar{X}^b)$ ),  
 31 where  $H$  is the observation forward operator that transforms values in the model space to





1 those in the observation space);  $\tilde{P}^a = \left[ (Y^b)^T R^{-1} Y^b + \frac{(K-1)I}{r} \right]^{-1}$  is the analysis error  
2 covariance matrix in ensemble space, which is a function of  $Y^b = HXb$ , the matrix of  
3 background ensemble perturbations in the observation space,  $R$ , the observation error  
4 covariance (e.g., measurement error, aggregation error, representation error), and of  $r$ , a  
5 multiplicative inflation parameter; and  $\tilde{K} = \tilde{P}^a Y^b R^{-1}$ . LETKF assimilates  
6 simultaneously all observations within a certain distance at each analysis grid point,  
7 which defines the localization scale. Hunt et al. [2004] introduced a 4-dimensional  
8 version, and Hunt et al. [2007] provide a detailed documentation of the 4D-LETKF  
9 which we are using.

10

#### 11 **2.4 Choosing the long observation window (OW) and the short assimilation window** 12 **(AW)**

13 Like other data assimilation methods, LETKF proceeds in analysis cycles that  
14 consist of two steps, a forecast step and an analysis step. In the analysis step, the model  
15 forecast (also called prior or background), and the observations, are optimally combined  
16 to produce the analysis (also called the posterior), which is the best estimate of the  
17 current state of the system under study. In the forecast step, the model is then advanced in  
18 time with the analysis as the initial condition and its result becomes the forecast for the  
19 next analysis cycle. The assimilation time window for a regular 4D-LETKF is the length  
20 of the forecast ~~step~~. All observations within the assimilation time window are used to  
21 constrain the state at the end of the assimilation window.

22 The focus in this study is on the estimation of SCFs that are time varying  
23 parameters in GEOS-Chem. As discussed earlier, a preliminary LETKF analysis, which  
24 provides the weights for each ensemble perturbation, is performed over a longer window  
25 (e.g., 7 days with observations starting at time  $t$ ). Then, the “No-Cost” smoothing  
26 [Kalnay et al, 2007b, Kalnay and Yang, 2010] is applied, using the same analysis weights  
27 obtained at the end of the long observation window (e.g., 7 days) for each ensemble  
28 member, but combining the ensemble perturbations at the end of the corresponding short  
29 assimilation window (e.g., 1-day). This creates the final 1-day analysis (at time  $t+AW$ ),  
30 which benefits from the information from all the observations made throughout the long  
31 OW (7 days), and from the linearity of the perturbations in the short AW of 1 day, which



1 is required for accuracy. At this time the procedure is repeated starting at  $t+AW$ , one day  
2 later.

3 In this new approach, we have the flexibility to combine a short assimilation  
4 window (AW) of length  $m$ , with a long observation window (OW) of length  $n$ , to  
5 improve the estimation of SCF. In the forecast step, the model is integrated from  $t$  to  $t+n$ ,  
6 to produce the forecast corresponding to the observations within the OW. In the analysis  
7 step, the observations and corresponding forecasts within the OW are used by the LETKF  
8 to estimate optimal weights for the ensemble members. The “No-Cost” smoother applies  
9 these optimal weights to determine the analysis of the model state and the SCF parameter  
10 at  $t + m$ . The resulting analysis is then used as the initial conditions for the next analysis  
11 cycle starting from time  $t + m$ .

12

### 13 **2.5 Experimental setup**

14 In our experiments we used an ensemble size of 20 members, which was  
15 optimal in the sense that increasing the number of ensemble members did not  
16 significantly improve the results. The initial ensemble is created by random selection of  
17 the state and flux values from the model-based “nature” run for both SCF and  
18 atmospheric CO<sub>2</sub> concentration. Therefore, the initial uncertainties of fluxes and CO<sub>2</sub>  
19 values are equivalent to their “natural” variability. Based on a sensitivity analysis, we  
20 found a horizontal localization radius of 150 km is optimal for our system. Following  
21 Kang et al. [2012], a vertical localization is also applied assigning a larger weight to the  
22 CO<sub>2</sub> updating on surface layers to reflect the expected dominance of layers near the  
23 ground in the change of the column total CO<sub>2</sub> measured by OCO-2.

24

### 25 **2.6 Additive Inflation Method**

26 The inflation is very important for our LETKF\_C data assimilation system. The  
27 LETKF uses the forecast ensemble spread to represent forecast uncertainties. All EnKFs  
28 tend to underestimate the uncertainty in their state estimate because of nonlinearities and  
29 limited number of ensemble members (Whitaker and Hamill, 2002). Underestimating the  
30 uncertainty (ensemble spread) leads to overconfidence in the background state estimate,  
31 and less confidence in the observations, which will eventually lead the EnKF to ignore



1 the observations and result in filter divergence. This is also true for our carbon-LEKF  
2 data assimilation system. The ensemble spread of CO<sub>2</sub> in GEOS-Chem model decreases  
3 during model integration when the ensemble members are using the same meteorological  
4 forcing and SCF values, which is very different from the system with prognostic  
5 meteorological fields with the ensemble spread of model state increasing during model  
6 integration (not shown). The ensemble spread of SCFs also does not increase during  
7 model integration because the SCFs are predicted using persistence. However, the  
8 LETKF decreases the ensemble spreads for both SCFs and CO<sub>2</sub> during analysis steps.  
9 Therefore, without inflation, the ensemble spread of the CO<sub>2</sub> and SCFs would be  
10 continuously decreasing during data assimilation, and soon would become too small for  
11 LETK to accept any observations, and hence, cause filter divergence.

12 There are different types of inflation methods that address the problem of  
13 overconfidence: multiplicative inflation, relaxation to prior, and additive inflation [e.g.  
14 Anderson and Anderson, 1999; Mitchell and Houtekamer, 2000; Zhang et al., 2004;  
15 Whitaker et al., 2008; Miyoshi, 2011]. For this study, we chose additive inflation, which  
16 adds random fields to the analysis before the ensemble forecast of the next analysis cycle.  
17 Additive inflation has some advantages compared to multiplicative inflation because it  
18 prevents the effective ensemble dimension from collapsing toward the dominant  
19 directions of error growth [Whitaker et al., 2008; Kalnay et al., 2007a]. We applied  
20 additive inflation to the ensemble of atmospheric CO<sub>2</sub> and SCF to increase perturbations  
21 in the initial conditions, for the next time step. Following Kang et al [2012], the added  
22 field for each ensemble member is selected randomly from the nature run. Pairs of  
23 atmospheric CO<sub>2</sub> and surface CO<sub>2</sub> flux fields are chosen randomly within one year  
24 before the analysis time and then scaled to a magnitude corresponding to 30% of their  
25 seasonal variance.

26

### 27 **3. Sensitivity analysis for AW and OW length**

28 We tested the new version of the LETKF with short AW and long OW, described  
29 in previous sections. To test this new technique, we conducted two sets of experiments  
30 using the LETKF\_C system in an OSSE framework with OCO-2 like observations. The  
31 first set of experiments used the regular 4D-LETKF settings (with a single window length



1 AW=OW) to investigate the effect of the length of AW for estimating SCF. In the second  
 2 set of experiments, we investigated the optimal OW length choosing the best AW from  
 3 the first set of experiments. The assimilation period for all experiments was 1 January  
 4 2015 to 1 March 2016. The annual mean RMSEs differences are calculated by removing  
 5 from the simulation results the spin-up period of first two months. The details of  
 6 experimental settings are shown in Table 1.

7

8 Table 1. Lengths of Assimilation Window (AW), and Observation Window (OW), and  
 9 the resulting mean RMSEs for different experiments. The first four experiments use  
 10 regular 4D-LETKF, with AW=OW. The last four experiments use AW=1 day, found to  
 11 be optimal, and different OWs.

	EXP1	EXP2	EXP3	EXP4	EXP5	EXP6	EXP7	EXP8
AW	6 hours	1 day	3 days	7 days	1 day	1 day	1 day	1 day
OW	6 hours	1 day	3 days	7 days	2 days	8 days	15 days	30 days
RMSE ( $\frac{kgC}{m^2 \cdot yr}$ )	0.077	<b>0.059</b>	0.068	0.074	0.053	<b>0.041</b>	<b>0.040</b>	0.050

12

13

#### 14 Sensitivity analysis for different assimilation windows

15 The sensitivity of SCF estimates to the length of AW was investigated based on  
 16 the first set of experiments (EXP1-EXP4) with regular 4D-LETKF settings, where the  
 17 length of OW is the same as that of the AW. All experiments used the same observations  
 18 and initial conditions. Since the coverage of OCO-2 observation network is too sparse  
 19 for our LETKF\_C assimilation system to estimate the SCF signal in a short time scales,  
 20 here we focus mainly on the estimation of SCF in the seasonal and longer time scale.

21 Figure 2 shows the estimated global total surface fluxes from the first set of  
 22 experiments. The “true” global total surface fluxes show a clear seasonal cycle with very  
 23 large carbon uptake during the growing season of Northern Hemisphere (NH), from May  
 24 to August, and carbon release during other seasons with the peak release during  
 25 November. All experiments reproduced fairly well the seasonal cycle of SCF.



1           When the AW is very short (6 hours), there are large magnitude and high  
2 frequency noise overlaying the seasonal cycle. The magnitude of high frequency errors of  
3 SCF estimation in EXP1 is comparable with the seasonal variability of SCF (Figure 2a).  
4 When the AW=7 days is selected, the high frequency errors of estimation decay, but the  
5 deviations of estimates from the “truth” increase. The EXP2 with AW= 1 day produced  
6 the best estimation of SCF among all four experiments with equal observation and  
7 assimilation windows (Figure 2).

8           The advantage of AW=1 day (EXP2) is clearly seen from the smaller average  
9 global root mean square error (RMSE) and from Figure 2c. The RMSE of surface carbon  
10 flux is calculated as

$$11 \quad RMSE(t) = \sqrt{E_x((F^a(x,t) - F^n(x,t))^2)} \quad (3)$$

12 where  $x$  and  $t$  are space and time location;  $F^a$  and  $F^n$  indicate the analysis and the “true”  
13 SCF from nature run, respectively.  $E_x$  is spatial average. The estimations from  
14 experiments with long AW (3 days and 7 days) have the smaller RMSE for the first 3  
15 months (January to March), when the “truth” had very little variation because the long  
16 AWs enhances the signal and smoothes the high-frequency noise. The experiments with  
17 long AW could miss the fine-scale signals of SCF variation and fail to catch its variation  
18 with time. Therefore, the estimations with long AW showed large RMSE during the  
19 period when the SCF had larger variations. The estimation with AW of 6 hour showed  
20 very large RMSE because of the overwhelming high frequency noise. The estimation  
21 with AW of 1 day had the smallest RMSE among all the experiments with regular 4D-  
22 LETKF.

23           The yearly mean RMSEs of SCFs showed very similar spatial patterns, but  
24 different amplitudes for different experiments (Figure 3). The large RMSEs of SCF  
25 estimation located in Southeast American, Southeast of China and Russia, and resembled  
26 that of the SCF variance (not shown). The regions of higher variance indicate more  
27 information is needed to resolve such large variance by observations, which is hard to  
28 achieve. As expected, the SCF RMSE of 0.059 from EXP2 with AW of 1 day is  
29 significantly smaller than the RMSE from EXP1 with a short AW of 6 hour ( $0.077 \frac{kgC}{m^2 \cdot yr}$ ),  
30 and EXP3 and EXP4 with longer AWs of 3 days ( $0.068 \frac{kgC}{m^2 \cdot yr}$ ) and 7 days ( $0.074 \frac{kgC}{m^2 \cdot yr}$ )



1 respectively.

2 Our results show that the preferred AW for estimating SCF is 1 day. This is  
3 distinctly different from previously published studies that indicate either a very short AW  
4 (6 hours) [Kang et al 2011, 2012], or a very long AW (longer than a few weeks) [e.g.,  
5 Baker et al. , 2006, 2010; Peters et al., 2005, 2007; Michalak, 2008; Feng et al., 2009]. A  
6 short AW can better constrain the model state and therefore produce a better parameter  
7 estimation. It is worth mentioning that a very short AW of 6 hours can degrade the SCF  
8 estimation with high frequency noise, in our LETKF-C system. We postulate that the  
9 high frequency noise is related to the sampling errors in the CO<sub>2</sub>-SCF covariance that has  
10 smaller signal-noise ratio compared to those in experiments with longer AWs.

11

## 12 **Sensitivity analysis for different observation windows (OW)**

13 The results presented earlier and associated discussion suggest that parameter  
14 estimation through data assimilation benefits from long training time and having  
15 sufficient number of observations, implying that the length of OW is critical for the  
16 estimation of desired parameter(s). We investigated this sensitivity to find the suitable  
17 length of OW for estimating SCF in the second set of experiments (EXP5-EXP8), all  
18 based on the optimum AW=1 day that was identified from the first set of experiments,  
19 with different OW lengths.

20 The estimated global total SCFs in the second set of experiments show a clear  
21 seasonal cycle matching the “truth” (Figure 4a). Compared with EXP2 (OW=1) shown  
22 with the green line in Figure 2a), EXP5 (OW=2days) reduced the high frequency noise  
23 significantly when the OW length was increased from 1 day to 2 days. There is still some  
24 high frequency noise in the SCF estimation for EXP5, because the observations for 2  
25 days are not sufficient to smooth out the high frequent noise introduced into the  
26 estimation through data assimilation. The estimated global total SCFs for EXP6  
27 (OW=8days), EXP7 (OW=15), EXP8 (OW=30) are much smoother than that of EXP5  
28 (OW=1day), because of their longer OW. However, the estimation for OW of 30 days  
29 shows a clear time shift compared with “truth”, especially during the transient period  
30 with the majority of plants switching from dormant phase in the winter to the growing  
31 phase in the spring. The surface carbon fluxes change rapidly during this period. The time



1 shift can also be seen in the estimations for these experiments with OW of 15 days, but it  
2 is less pronounced. In the LETKF technique, most of observations in a long OW are  
3 introduced at a time later than the assimilation time. Since the SCFs are temporal  
4 evolving parameters, the information (variation) of future surface fluxes is brought into  
5 the estimation of current time when the future observations are included in the OW.  
6 Therefore, the estimated SCF with a very long OW tend to shift towards its future value.  
7 The estimated SCF with moderate OW=8 days and 15 days (EXP6 and EXP7) are more  
8 accurate than those with a short OW of 2 days (EXP5) and very long OW of 30 days  
9 (EXP8), by avoiding the significant high frequent noise observed in EXP5 (OW=2 days)  
10 and severe time shift present in EXP8 (OW=30 days). The global mean RMSEs of  
11 estimated SCF from OW=8 and 15 days (EXP6 and EXP7) are significantly smaller than  
12 those from OW=2 and 30 days, i.e., EXP5 and EXP8 (Figure 4c).

13 The spatial pattern of annual average RMSE of SCF for EXP5 (OW=2 days;  
14 Figure 5) is similar to those in the first set of experiments, which had short AW=OW  
15 (Figure 3). The regions with large RMSE in EXP5 (OW=2 days) disappear with OW=7  
16 and 15 days in EXP6 and EXP7, because the long OWs enhance the signals for SFC  
17 estimation. The large RMSE in SCF estimates for EXP8 (OW=30 days) are primarily in  
18 the Northern Hemisphere mid-latitudes, because of the time shift in estimations with  
19 OW=30 days. The mean RMSEs of experiments with moderate OWs of 8 and 15 days  
20 are  $0.041 \frac{kgC}{m^2yr}$  and  $0.040 \frac{kgC}{m^2yr}$ , respectively, which is significantly smaller than those  
21 from experiments with OWs of 2 days ( $0.053 \frac{kgC}{m^2yr}$ ) and 30 days ( $0.050 \frac{kgC}{m^2yr}$ ).

22 A longer OW requires a longer forecast period for each forecast step, which  
23 results in additional computational time/cost. For example, EXP7 with OW of 8 days  
24 used 8-time more computational time for its estimation compared to EXP2. Furthermore,  
25 the length of OW is also constrained by the time scale of estimation parameters. A long  
26 OW tends to generate a time shift for its estimation. For seasonal and longer time scales,  
27 OW(s) in moderate range of 8~15 days appear to be most suitable for the LETKF\_C  
28 estimates of the SCF. EXP7 and EXP8 show almost the same quality of SCF estimation,  
29 but EXP7 has higher computational efficiency. The best configuration thus appears to be  
30 EXP7 with an OW of 8 days and AW of 1 day, referred as the “benchmark” experiment





1 hereafter.

2 We note that the high frequency noise in EXP1 with a short AW of 6 hours can be  
3 smoothed out by a long OW (i.e. 8-15 days). We speculate that an experiment with AW  
4 of 6 hours and OW 8 days will produce similarly realistic estimations as the “benchmark”  
5 experiment; however, it requires much more computational time.

6

### 7 **5 Evaluating estimated fluxes from the “benchmark” experiment**

8 With the moderate long observation and short assimilation windows, we obtained  
9 best estimates of surface carbon fluxes, and their seasonal cycle. This section describes  
10 the SCF estimates from the “benchmark” experiment. Figure 6 shows a comparison of  
11 surface carbon fluxes based on the “benchmark” assimilation experiment and nature  
12 (“truth”) run for Northern Hemisphere Summer and Winter seasons. The “bottom-up”  
13 carbon fluxes used in the “nature” run show a very strong seasonal cycle over the  
14 continents, except Antarctica. The North Hemisphere mid-latitude areas are very large  
15 carbon sinks in the Summer, and carbon sources in the Winter. The strong seasonal cycle  
16 of surface fluxes mainly related to the variability of terrestrial ecosystems that absorbs  
17 large amount of CO<sub>2</sub> during the growing season (Spring and Summer) and release carbon  
18 back to the atmosphere during dormant seasons (Fall and Winter). The estimated surface  
19 fluxes in the seasonal time scale follow closely the “truth”. The benchmark assimilation  
20 experiment closely reproduces the spatial pattern of surface fluxes globally, for different  
21 seasons. The difference between the benchmark estimation and “truth” shown in Figures  
22 6 d & f are very small. There are positive carbon fluxes over Northern Hemisphere mid-  
23 latitudes in the Winter, thus a positive bias in estimated atmospheric CO<sub>2</sub> concentration  
24 is expected.

25 A successful estimation of surface fluxes requires a good assimilation of atmospheric  
26 CO<sub>2</sub>, and a good estimation of surface flux parameters helps the model-assimilation  
27 system to produce a good analysis of atmosphere CO<sub>2</sub>. Figure 7 shows the comparison of  
28 surface atmospheric CO<sub>2</sub> concentrations between the benchmark assimilation experiment  
29 and nature (“truth”) run for Northern Hemisphere Summer and Winter. The spatial  
30 pattern of assimilated CO<sub>2</sub> matches the “truth” very well. The analysis successfully  
31 reproduced the seasonal cycle of CO<sub>2</sub> over Northern Hemisphere mid-latitudes, with low





1 CO<sub>2</sub> concentration in Summer (Figures 7a-c) and high CO<sub>2</sub> in Winter (Figures 7b-d),  
2 consistent with seasonal cycle of CO<sub>2</sub> absorption and release by terrestrial ecosystems.  
3 There are positive CO<sub>2</sub> concentrations located at high latitudes of North America and far  
4 East Asia regions during Winter 2016 (Figure 7f), due to the positive bias in estimated  
5 SCF (Figure 6f).

6 The consistency of annual mean estimated SCF for both benchmark experiment  
7 and “truth” is a very important feature for our LETKF\_C assimilation system (Figure 8a).  
8 In EnKF assimilation the ensemble spread is considered as a good representation of  
9 uncertainties associated with both parameters and model state [e.g., Evensen 2007, Liu et  
10 al. 2014]. The surface carbon fluxes are special parameters that vary with time and it is  
11 very hard to quantify their uncertainty during assimilation. When the ensemble spread of  
12 parameters are too small to drive model with a robust response, the estimation fails. The  
13 additive inflation with 30% of nature variability is used to maintain the amplitude of  
14 parameters ensemble spread. Although the ensemble spread of the global total surface  
15 flux, in our experiments, is bigger than its error (Figure 8a), we still estimated very well  
16 the global total surface CO<sub>2</sub> fluxes (ensemble mean), and their seasonal variability. This  
17 is consistent with findings of Liu et al [2014], that parameter estimation can tolerate some  
18 inconsistency between parameter ensemble spread and parameter error.

19 The global mean RMSE of SCF decrease from an initial value of ~0.1  
20  $kg\ C\ m^{-2}y^{-1}$  to ~0.04  $kg\ C\ m^{-2}y^{-1}$  in just a few analysis cycles (Figure 8b). It does  
21 not further decrease during assimilation because the SCF values vary temporally. The  
22 signals added by observations are mainly used to reproduce the temporal variation of  
23 SCF.

24 It is very important for a SCF estimation to reproduce the spatial distribution of  
25 the annual mean of the SCF, since it identifies the carbon sources and sinks in the Earth  
26 System. Though the amplitude of annual mean SCF is much smaller than the seasonal  
27 cycle of SCF, the estimated spatial pattern of annual mean SCF in the benchmark  
28 experiment (Eq. 4) is generally consistent with the “truth” (Figure 9).

$$29 \Delta F(x) = E_t(F^a(x, t)) - E_t(F^n(x, t)) \quad (4)$$

30 In summary, we found that the OSSE experiments using long observation  
31 windows and short assimilation windows resulted in the best estimates of SCF.



1

## 2 **6 Summary and Conclusions**

3           We have developed a LETKF-GEOS-Chem carbon data assimilation (LETKF\_C)  
4 system to estimate the surface carbon fluxes (SCF). The GEOS-Chem is run by the  
5 single realization of reanalysis meteorology fields driven by MERRA. The SCF vary  
6 spatially and temporally in the system.

7           The LETKF requires a short assimilation window to avoid an ill-posed condition  
8 caused by the nonlinear processes in the forecast model with a long forecast time. The  
9 parameter estimation favors a long training period and many observations. Based on  
10 these features, we developed a new method to accurately estimate the SCF. The new  
11 scheme separates original assimilation time window into observation (OW) and  
12 assimilation (AW) windows, allowing the flexibility to apply an OW that is different than  
13 the AW. Like RIP, the new technique takes advantage of the “no-cost smoothing”  
14 algorithm developed for the LETKF by Kalnay et al. [2007b] that allows to translate the  
15 Kalman Filter solution forward or backward within the observation window.

16           The new method was applied to the LETKF\_C system in the OSSE mode using a  
17 dataset developed based on the OCO-2 observation characteristics. The sensitivity  
18 experiments for this model-assimilation system demonstrated that the new technique,  
19 with a short AW and long OW, significantly improves the SCF estimation as  
20 compared to regular 4D-LETKF with identical observation and assimilation windows.  
21 The best AW for SCF estimation is 1 day, which is different from the typical AW of 6  
22 hours used in the meteorological assimilations. An OW in the range of 8-15 days is  
23 required to estimate the surface carbon fluxes for seasonal and longer time scales. The  
24 benchmark experiment with AW of 1 day and the OW of 8 days successfully reproduced  
25 the mean seasonal and annual SCF. The newly developed assimilation method can be  
26 used with other Earth system models, especially for greater use of observations in  
27 conjunction with models.

28

## 29 **Code and data availability**

30           This work focuses on developing new methodology for the estimation of carbon  
31 flux using carbon cycle data assimilation. It does not generate any new data set. The



1 related code for GEOS-Chem and LETKF can be access on  
2 [http://acmg.seas.harvard.edu/geos/doc/man/chapter\\_2.html#DownCode](http://acmg.seas.harvard.edu/geos/doc/man/chapter_2.html#DownCode) and  
3 <https://github.com/takemasa-miyoshi/letkf>, respectively.

4 **References:**

- 5 Anderson JL. (2001), An ensemble adjustment Kalman filter for data assimilation. *Mon.*  
6 *Wea. Rev.*, 129, 2884–2903.
- 7 Anderson JL. (2003), A local least squares framework for ensemble filtering. *Mon. Wea.*  
8 *Rev.*, 131, 634–642.
- 9 Anderson, J. L., and S. L. Anderson (1999), A Monte Carlo implementation of the  
10 nonlinear filtering problem to produce ensemble assimilations and forecasts, *Mon.*  
11 *Weather Rev.*, 127, 2741–2758,  
12 doi:10.1175/15200493(1999)127<2741:AMCIOT>2.0.CO;2.
- 13 Asefi-Najafabady, S., P. J. Rayner, K. R. Gurney, A. McRobert, Y. Song, K. Coltin, J.  
14 Huang, C. Elvidge, and K. Baugh (2014), A multiyear, global gridded fossil fuel CO<sub>2</sub>  
15 emission data product: Evaluation and analysis of results, *J. Geophys. Res. Atmos.*, 119,  
16 10,213–10,231, doi:10.1002/2013JD021296.
- 17 Banks, H.T. (1992a), Control and estimation in distributed parameter systems. In:  
18 H.T. Banks, Editor, *Frontiers in Applied Mathematics* vol. 11, SIAM, Philadelphia, pp  
19 227.
- 20 Banks, H.T. (1992b), Computational issues in parameter estimation and feedback control  
21 problems for partial differential equation systems. *Physica D* 60, 226-238.
- 22 Baker, D. F., S. C. Doney, and D. S. Schimel (2006), Variational data assimilation for  
23 atmospheric CO<sub>2</sub>, *Tellus, Ser. B*, 58, 359–365, doi:10.1111/j.1600-0889.2006.00218.x.
- 24 Baker, D. F., H. Bösch, S. C. Doney, D. O’Brien, and D. S. Schimel (2010), Carbon  
25 source/sink information provided by column CO<sub>2</sub> measurements from the Orbiting  
26 Carbon Observatory, *Atmos. Chem. Phys.*, 10, 4145–4165, doi:10.5194/acp-10-4145-  
27 2010.
- 28 Bey, I., D. J. Jacob, R. M. Yantosca, J. A. Logan, B. Field, A. M. Fiore, Q. Li, H. Liu, L.  
29 J. Mickley, and M. Schultz (2001), Global modeling of tropospheric chemistry with  
30 assimilated meteorology: Model description and evaluation, *J. Geophys. Res.*, 106,  
31 23,073-23,096.



- 1 Nassar, R., L. Napier-Linton, K.R. Gurney, R.J. Andres, T. Oda, F.R. Vogel, and F. Deng  
2 (2013), Improving the temporal and spatial distribution of CO<sub>2</sub> emissions from global  
3 fossil fuel emission data sets, *J. Geophys. Res. Atmos.*, 118, 917-933,  
4 doi:10.1029/2012JD018196.
- 5 Bishop CH, Etherton BJ, and Majumdar SJ. (2001), Adaptive sampling with the  
6 ensemble transformation kalman filter. Part i: theoretical aspects. *Mon. Wea. Rev.*, 129,  
7 420–436
- 8 Bosilovich MG, Akella S, Coy L et al. (2015) MERRA-2: Initial evaluation of the  
9 climate. Series on Global Modeling and Data Assimilation, NASA/TM, 104606.
- 10 Burgers G, Van Leeuwen P, Evensen G. (1998), Analysis scheme in the ensemble  
11 Kalman filter. *Mon. Wea. Rev.*, 126, 1719–1724.
- 12 Chevallier, F., R. J. Engelen, C. Carouge, T. J. Conway, P. Peylin, C. Pickett-Heaps, M.  
13 Ramonet, P. J. Rayner, and I. Xueref-Remy (2009), AIRS-based versus flask-based  
14 estimation of carbon surface fluxes, *J. Geophys. Res.*, 114, D20303,  
15 doi:10.1029/2009JD012311.
- 16 Cooperative Global Atmospheric Data Integration Project (2016), Multi-laboratory  
17 compilation of atmospheric carbon dioxide data for the period 1957-2015;  
18 obspack\_co2\_1\_GLOBALVIEWplus\_v2.1\_2016\_09\_02; NOAA Earth System Research  
19 Laboratory, Global Monitoring Division. <http://dx.doi.org/10.15138/G3059Z>
- 20 Crisp, D., et al. (2004), The Orbiting Carbon Observatory (OCO) mission, *Adv. Space*  
21 *Res.*, 34, 700–709, doi:10.1016/j.asr.2003.08.062.
- 22 Evensen G. (1994), Sequential data assimilation with a non-linear quasi-geostrophic  
23 model using Monte Carlo methods to forecast error statistics. *J. Geophys. Res.*, 99(C5),  
24 10143–10162.
- 25 Enting, I. G. (2002), *Inverse Problems in Atmospheric Constituent Transport*, Cambridge  
26 Univ. Press, New York, doi:10.1017/CBO9780511535741.
- 27 Feng, L., P. I. Palmer, H. Bösch, and S. Dance (2009), Estimating surface CO<sub>2</sub> fluxes  
28 from space-borne CO<sub>2</sub> dry air mole fraction observations using an ensemble Kalman  
29 filter, *Atmos. Chem. Phys.*, 9, 2619–2633, doi:10.5194/acp-9-2619-2009.
- 30 HARLIM, J. and HUNT, B. R. (2007), Four-dimensional local ensemble transform  
31 Kalman filter: numerical experiments with a global circulation model. *Tellus A*, 59: 731–



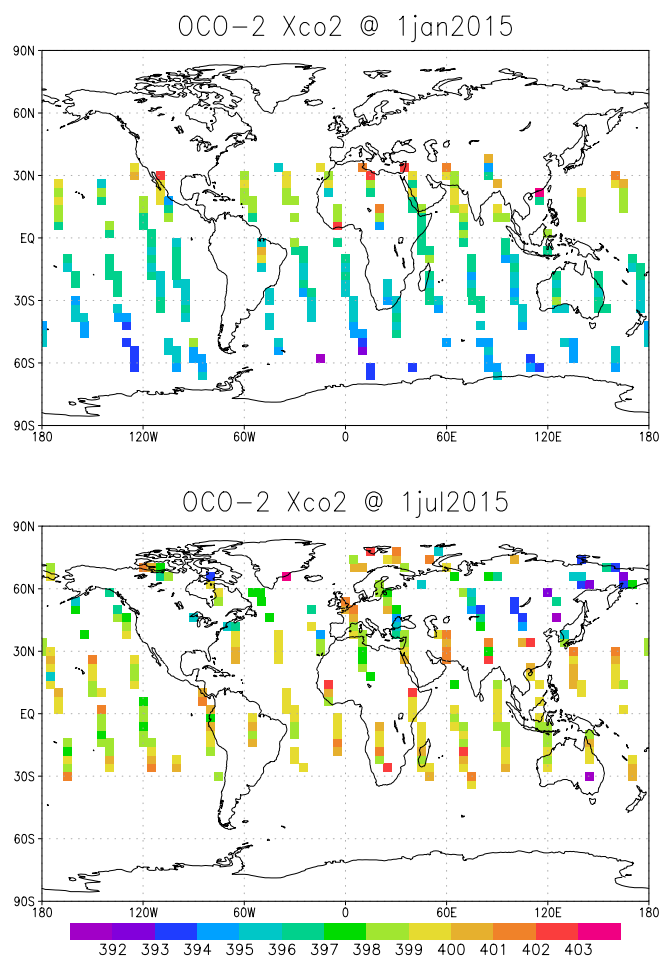
- 1 748. doi:10.1111/j.1600-0870.2007.00255.x
- 2 Houtekamer PL, Mitchell HL. (1998), Data assimilation using an ensemble Kalman filter  
3 technique. *Mon. Wea. Rev.*, 126, 796–811.
- 4 Hunt, B. R., E. Kostelich, and I. Szunyogh (2007), Efficient data assimilation for  
5 spatiotemporal chaos: A local ensemble transform Kalman filter, *Physica D*, 230, 112–  
6 126, doi:10.1016/j.physd.2006.11.008.
- 7 Liu Y, Liu Z, Zhang S, Jacob R, Lu F, Rong X, Wu S (2014), Ensemble-Based Parameter  
8 Estimation in a Coupled General Circulation Model. *Journal of climate*, 27, 7151–7162.
- 9 Le Quéré, C., Moriarty, R., Andrew, et al. (2015), Global carbon budget 2014, *Earth*  
10 *Syst. Sci. Data*, 7, 47-85, doi:10.5194/essd-7-47-2015.
- 11 Le Quéré C, Andrew RM, Canadell JG et al. (2016), Global Carbon Budget 2016, *Earth*  
12 *Syst. Sci. Data*, 8, 605-649, doi:10.5194/essd-8-605-2016.
- 13 Lokupitiya, R. S., D. Zupanski, A. S. Denning, S. R. Kawa, K. R. Gurney, and M.  
14 Zupanski (2008), Estimation of global CO<sub>2</sub> fluxes at regional scale using the maximum  
15 likelihood ensemble filter, *J. Geophys. Res.*, 113, D20110, doi:10.1029/2007JD009679.
- 16 Kalnay E., H. Li, T. Miyoshi, S.-C. Yang, and J. Ballabrera-Poy (2007a), 4-D-Var or  
17 ensemble Kalman filter?. *Tellus, Ser. A*, 59, 758–773, doi:10.1111/j.1600-  
18 0870.2007.00261.x.
- 19 Kalnay E., H. Li, T. Miyoshi, S.-C. Yang, and J. Ballabrera-Poy (2007b), Response to the  
20 discussion on “4-D-Var or EnKF?” by Nils Gustafsson. *Tellus, Ser. A*, 59, 778-780, doi:  
21 10.1111/j.1600-0870.2007.00263.x.
- 22 Kalnay, E. and Yang, S.-C. (2010), Accelerating the spin-up of Ensemble Kalman  
23 Filtering. *Q.J.R. Meteorol. Soc.*, 136: 1644–1651. doi:10.1002/qj.652
- 24 Kang, J.-S., E. Kalnay, J. Liu, I. Fung, T. Miyoshi, and K. Ide (2011), “Variable  
25 localization” in an ensemble Kalman filter: Application to the carbon cycle data  
26 assimilation, *J. Geophys. Res.*, 116, D09110, doi:10.1029/2010JD014673.
- 27 Kang J.-S., Kalnay E, Miyoshi T, Liu J, Fung I (2012), Estimation of surface carbon  
28 fluxes with an advanced data assimilation methodology: SURFACE CO<sub>2</sub> FLUX  
29 ESTIMATION. *Journal of geophysical research*, 117.
- 30 Mitchell, H. L., and P. L. Houtekamer, (2000), An adaptive ensemble Kalman filter.  
31 *Mon. Wea. Rev.*, 128, 416–433.



- 1 Michalak, A. M. (2008), Adapting a fixed-lag Kalman smoother to a geostatistical  
2 atmospheric inversion framework, *Atmos. Chem. Phys.*, 8, 6789–6799.
- 3 Miyoshi, T. (2011), The Gaussian approach to adaptive covariance inflation and its  
4 implementation with the local ensemble transform Kalman filter. *Mon. Wea.*  
5 *Rev.*, 139, 1519–1535, doi:10.1175/2010MWR3570.1.
- 6 Kang, J.-S., E. Kalnay, T. Miyoshi, J. Liu, and I. Fung (2012), Estimation of surface  
7 carbon fluxes with an advanced data assimilation methodology, *J. Geophys. Res.*, 117,  
8 D24101, doi:10.1029/2012JD018259.
- 9 Peters, W., J. B. Miller, J. Whitaker, A. S. Denning, A. Hirsch, M. C. Krol, D. Zupanski,  
10 L. Bruhwiler, and P. P. Tans (2005), An ensemble data assimilation system to estimate  
11 CO<sub>2</sub> surface fluxes from atmospheric trace gas observations, *J. Geophys. Res.*, 110,  
12 D24304, doi:10.1029/2005JD006157.
- 13 Peters, W., et al. (2007), An atmospheric perspective on North American carbon dioxide  
14 exchange: Carbon tracker, *Proc. Natl. Acad. Sci. U. S. A.*, 104, 18,925–18,930,  
15 doi:10.1073/pnas.0708986104.
- 16 Tippett M, Anderson JL, Bishop CH, Hamill TM, Whitaker JS. (2003), Ensemble square  
17 root filters. *Mon. Wea. Rev.*, 131, 1485–1490.
- 18 Wang, S., M. Xue, A. D. Schenkman, and J. Min (2013), An iterative ensemble square root  
19 filter and tests with simulated radar data for storm scale data assimilation. *Quart. J. Roy.*  
20 *Meteor. Soc.*, 139, 1888–1903.
- 21
- 22 Whitaker JS, Hamill TM. (2002), Ensemble data assimilation without perturbed  
23 observations. *Mon. Wea. Rev.*, 130, 1913–1924.
- 24 Whitaker JS, X. Wei, Y. Song, and Z. Toth (2008), Ensemble data assimilation with the  
25 NCEP global forecast system. *Mon. Wea. Rev.*, 136, 463–482.
- 26 Yang, S., E. Kalnay, and T. Miyoshi (2012), Accelerating the EnKF Spinup for Typhoon  
27 Assimilation and Prediction. *Wea. Forecasting*, 27, 878–897,  
28 <https://doi.org/10.1175/WAF-D-11-00153.1>
- 29
- 30 Yokota, T., H. Oguma, I. Morino, and G. Inoue (2004), A nadir looking SWIR FTS to  
31 monitor CO<sub>2</sub> column density for Japanese GOSAT project, in *Proceedings of the*  
32 *Twenty-fourth International Symposium on Space Technology and Science (Selected*

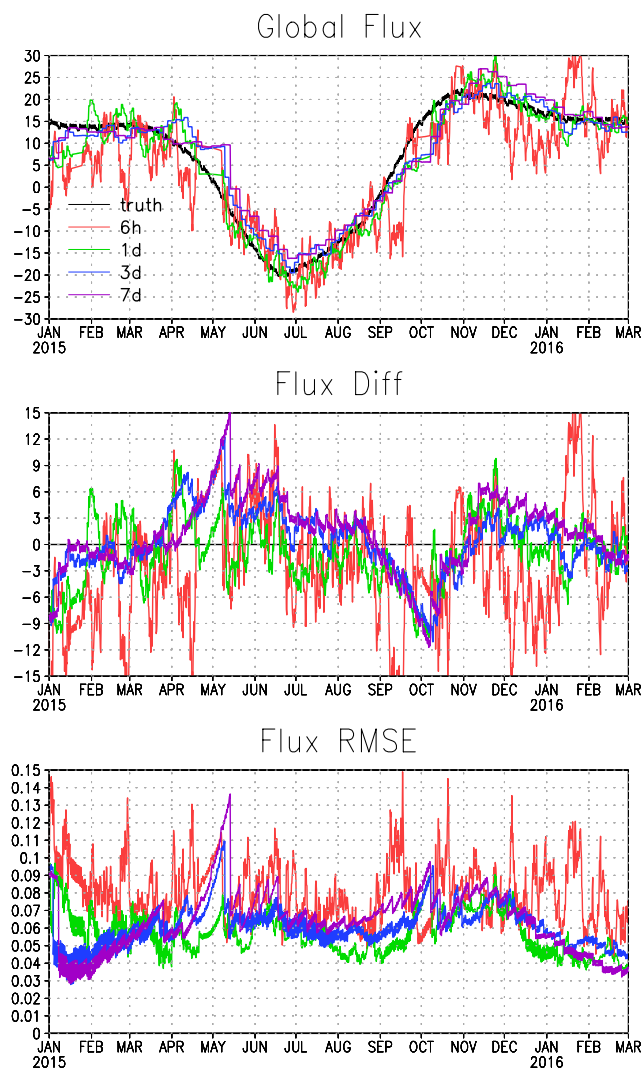


- 1 Papers), pp. 887–889, Jpn. Soc. for Aeronaut. and Space Sci., Tokyo.
- 2 Zeng, N., A. Mariotti, and P. Wetzel (2005), Terrestrial mechanisms of interannual CO<sub>2</sub>
- 3 variability, *Global Biogeochemical Cycles*, 19, GB1016, doi:10.1029/2004GB002273.
- 4 Zeng, N., H. Qian, E. Munoz, and R. Iacono (2004), How strong is carbon cycle-climate
- 5 feedback under global warming? *Geophys. Res. Lett.*, 31 L20203,
- 6 doi:10.1029/2004GL020904.]
- 7 Zhang, F., C. Snyder, and J. Sun (2004), Impacts of initial estimate and observation
- 8 availability on convective-scale data assimilation with an ensemble Kalman filter. *Mon.*
- 9 *Wea. Rev.*, 132, 1238–1253
- 10 Zupanski, D., A. S. Denning, M. Uliasz, M. Zupanski, A. E. Schuh, P. J. Rayner, W.
- 11 Peters, and K. D. Corbin (2007), Carbon flux bias estimation employing Maximum
- 12 Likelihood Ensemble Filter (MLEF), *J. Geophys. Res.*, 112, D17107,
- 13 doi:10.1029/2006JD008371.

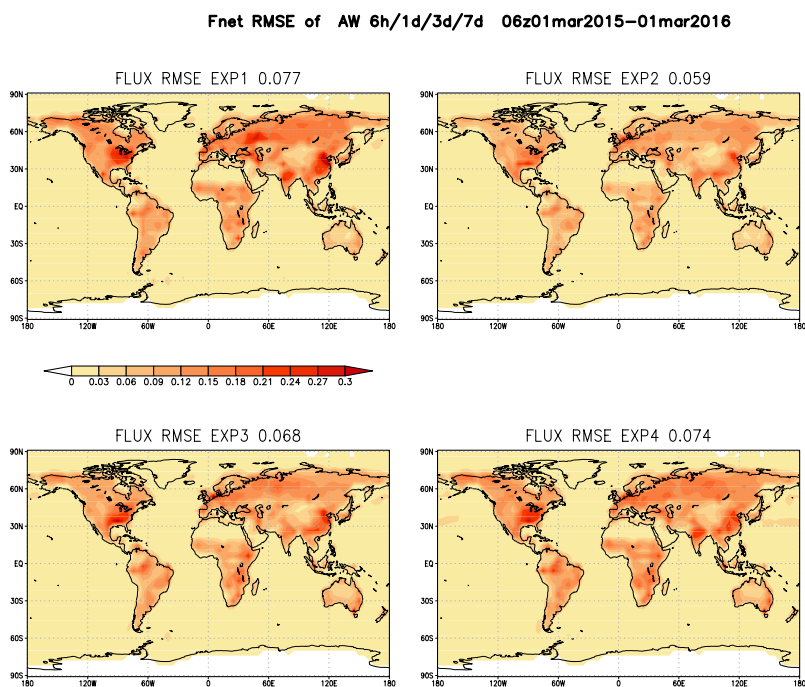


1  
2 Figure1 The 10-second average of good quality OCO-2 Xco2 observations (Warning  
3 Level  $\leq 15$ ), obtained from David Baker for 1 January 2015 (top panel) and 1 July  
4 2015 (lower panel).  
5  
6





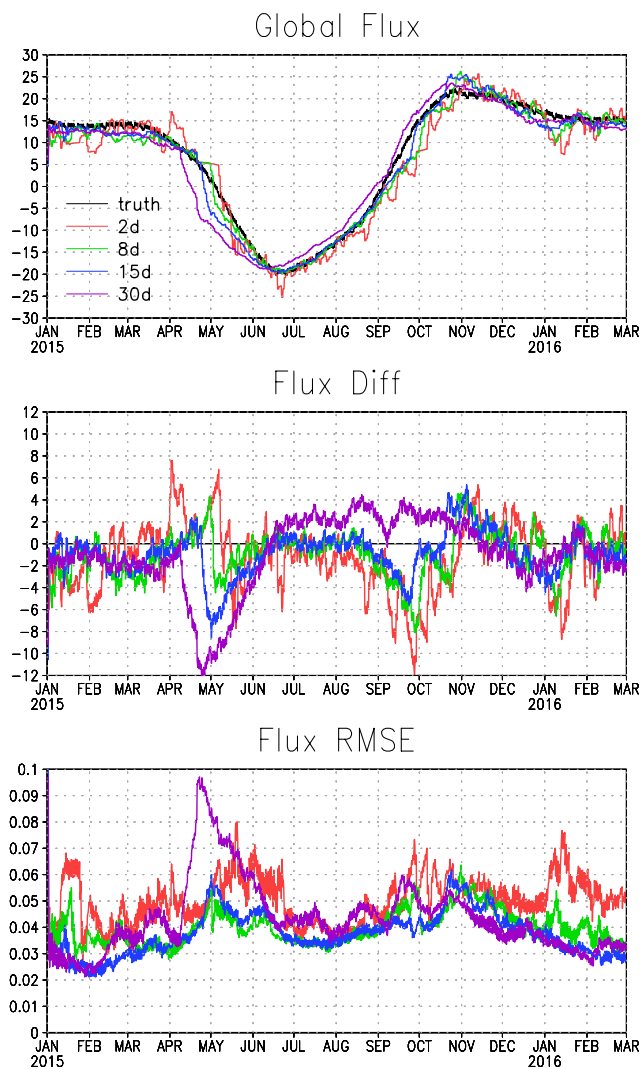
1  
2 Figure 2 Upper panel: the global total SCF from nature run (“truth”, black line) and  
3 from the estimations of the first set of experiments with different AW. Middle Panel:  
4 the difference of global total SCF between the estimations from the experiments  
5 with different AW and the nature run (“truth”). Lower panel: the global average  
6 RMSE of the estimated SCFs from the experiments with different AW.  
7



1  
2 Figure 3 The spatial pattern of the annual mean RMSE of estimated SCF from the  
3 experiments with different AW (EXP1-4).  
4  
5  
6



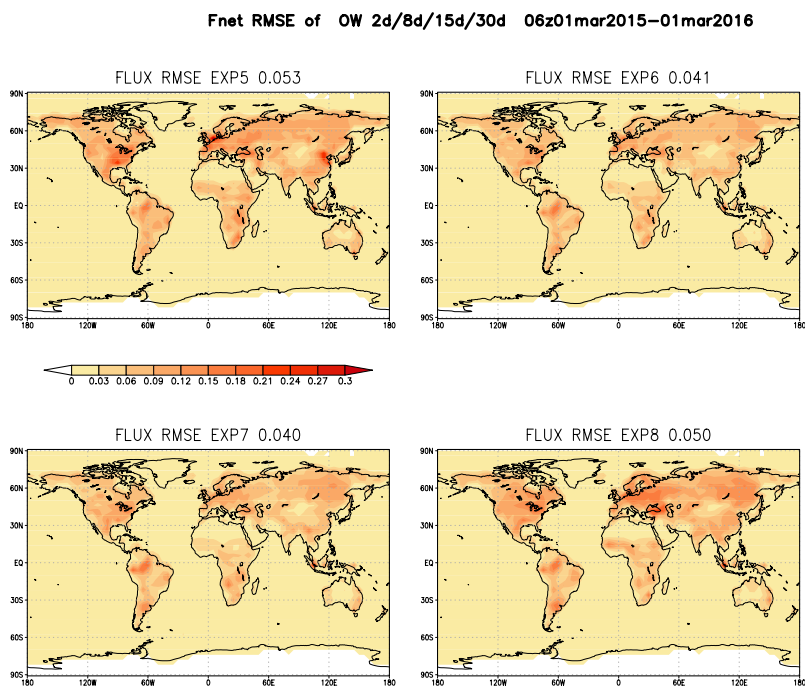
1



2  
3 Figure 4 Same as Figure 2, except for the second set of experiments with different  
4 OW, but same AW of 1 day.  
5



1

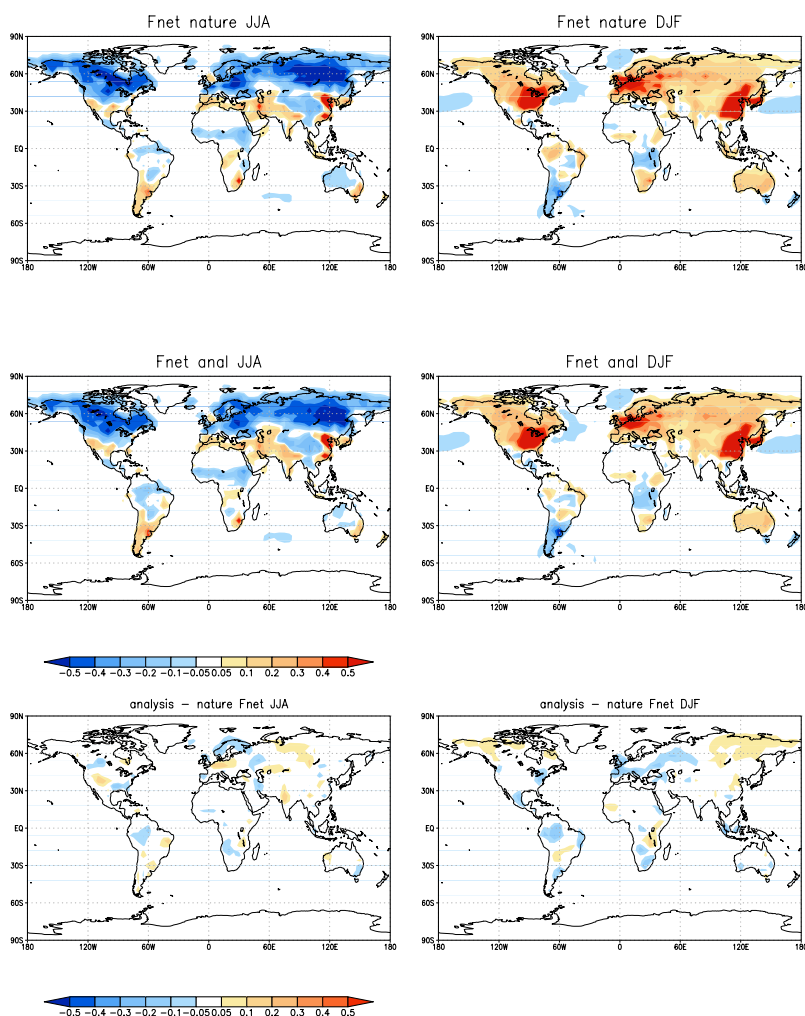


2  
3

4 Figure 5 Same as Figure 3, except for the second set of experiments with different  
5 OW, but similar AW of 1 day.



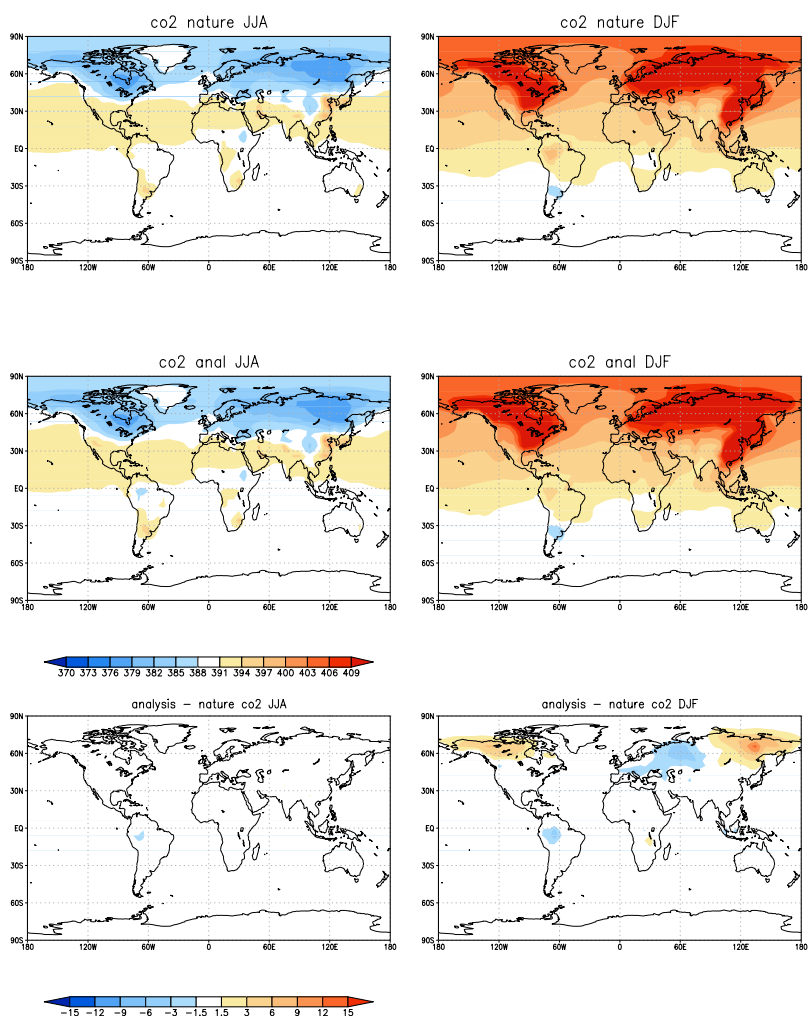
1



2  
3 Figure 6: The SCF of “nature” run and estimation from benchmark experiment for  
4 Northern Hemisphere Summer (left panels), and Winter (right panels).The top  
5 panels are the “truth” from the “nature” run; the middle panels are the estimates  
6 from benchmark experiment; and the lower panels are the difference between  
7 estimation and “truth”.

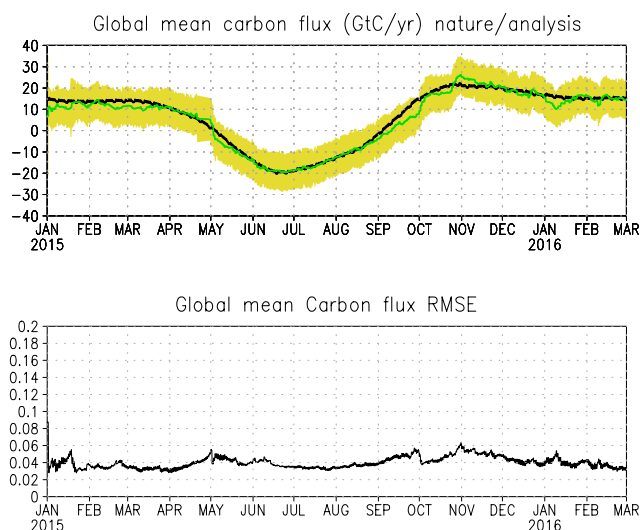


1



2  
3  
4

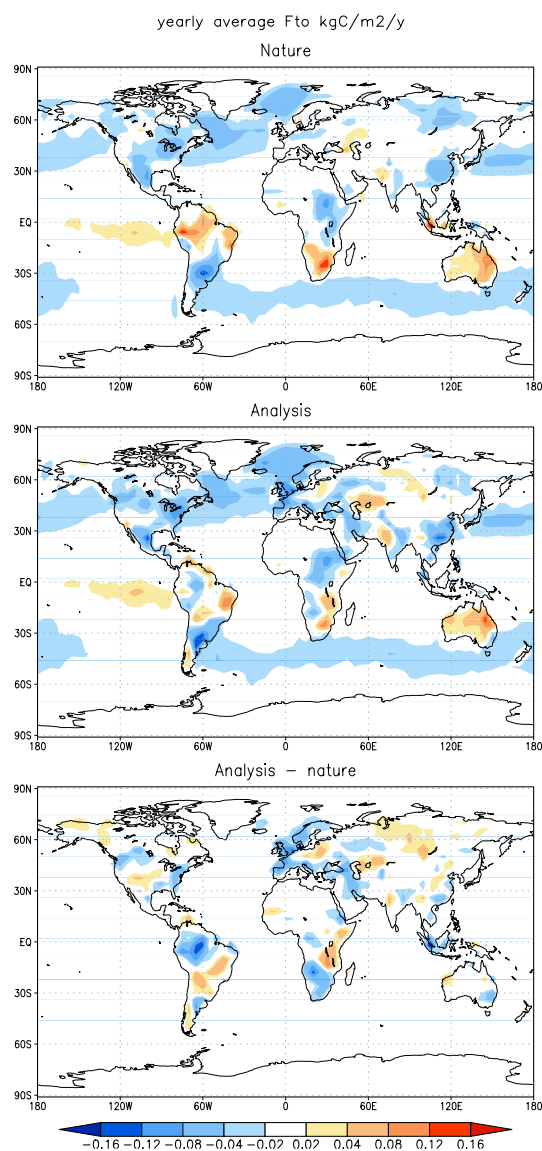
Figure 7. Same as Figure 6, except for surface concentrations of CO<sub>2</sub>



1  
2 Figure 8. The global total SCF of “truth” and estimation from the benchmark  
3 experiment (upper panel);the black line is the truth, green line is the ensemble  
4 mean of the estimation, and yellow shading is the ensemble spread. The global mean  
5 RMSE of the estimated SCF from the benchmark experiment is presented in the  
6 lower panel.



1



2  
3 Figure 9. The annual mean of SCF (with the FFE removed) for “nature” run (upper  
4 panel); the annual mean of estimated SCF (with the FFE removed) from benchmark  
5 experiment (middle panel); and their differences (lower panel)